Journal of Neurochemistry, 2006, **99**, 29–41 doi:10.1111/j.1471-4159.2006.04080.x

A rapid exocytosis mode in chromaffin cells with a neuronal phenotype

Alvaro O. Ardiles,* Jaime Maripillán,* Verónica L. Lagos,* Rodrigo Toro,* Italo G. Mora,* Lorena Villarroel,† Eva Alés,‡ Ricardo Borges§ and Ana M. Cárdenas*

**Centro de Neurociencia de Valparaíso, Universidad de Valparaíso, Chile*

†Departamento de Biología, Facultad de Ciencias, Universidad de Valparaíso, Chile

‡Departamento de Fisiología, Universidad de Sevilla, Spain

§Unidad de Farmacología, Universidad de La Laguna, Tenerife, Spain

Abstract

We have used astrocyte-conditioned medium (ACM) to promote the transdifferentiation of bovine chromaffin cells and study modifications in the exocytotic process when these cells acquire a neuronal phenotype. In the ACM-promoted neuronal phenotype, secretory vesicles and intracellular Ca^{2+} rise were preferentially distributed in the neurite terminals. Using amperometry, we observed that the exocytotic events also occurred mainly in the neurite terminals, wherein the individual exocytotic events had smaller quantal size than in undifferentiated cells. Additionally, duration of pre-spike current was significantly shorter, suggesting that ACM also modifies the fusion pore stability. After long exposure (7–9 days) to ACM, the kinetics of catecholamine release from individual vesicles was markedly accelerated. The morphometric analysis of vesicle diameters suggests that the rapid exocytotic events observed in neurites of ACM-treated cells correspond to the exocytosis of large dense-core vesicles (LDCV). On the other hand, experiments performed in EGTA-loaded cells suggest that ACM treatment promotes a better coupling between voltage-gated calcium channels (VGCC) and LDCV. Thus, our findings reveal that ACM promotes a neuronal phenotype in chromaffin cells, wherein the exocytotic kinetics is accelerated. Such rapid exocytosis mode could be caused at least in part by a better coupling between secretory vesicles and VGCC.

Keywords: astrocytes, catecholamines, chromaffin cells, exocytosis, neurotrophic factors, large dense-core vesicles.
J. Neurochem. (2006) **99**, 29–41.

Adrenal chromaffin cells have been employed as an experimental model to explore the exocytotic process (Burgoyne and Morgan 1998). In culture conditions, they have been used for real time measurements of exocytosis using techniques such as amperometry (Wightman *et al*. 1991). However, there are several striking differences between exocytosis in chromaffin cells and neurons, in particular regarding calcium sensitivity and kinetics (Burgoyne and Morgan 1998; Martin 2003). Further, the distribution of calcium channels in round-shaped chromaffin cells is different from that of neurons: In neurons, synaptic vesicles and voltage-gated Ca^{2+} channels (VGCC) are tightly coupled in the active zones (Llinas *et al*. 1995) whereas in chromaffin cells, VGCC are randomly distributed (Klingauf and Neher 1997; Gutierrez *et al*. 1998; Gil *et al*. 2001). The colocalization of VGCC and vesicles could be an important factor in determining the differences in exocytosis of neuroendocrine cells and neurons.

Adrenal chromaffin cells, like sympathetic neurons, derive from neural crest sympathoadrenal precursors (Patterson 1990). During development, the presence of substances such as glucocorticoids from the adrenal cortex inhibits neuronal differentiation of the precursors and induces a chromaffin phenotype (Doupe *et al*. 1985). Interestingly, chromaffin

Received April 11, 2006; revised manuscript received May 12, 2006; accepted May 12 , 2006.

Address correspondence and reprint requests to Ana M. Cárdenas, Centro de Neurociencia de Valparaíso, Universidad de Valparaíso, Chile. E-mail: ana.cardenas@uv.cl

Abbreviations used: ACM, astrocyte conditioned medium; bFGF, basic fibroblast growth factor; BSA, bovine serum albumin; CNTF, ciliary neurotrophic factor; DBH, dopamine β-hydroxylase; DMEM, Dulbecco's modified Eagle's medium; GDNF, glial cell line-derived neurotrophic factor; LDCV, large dense-core vesicles; NGF, nerve growth factor; PBS, phosphate-buffered saline; SNARE, SNAP receptors; VGCC, voltage-gated Ca^{2+} channels; SCV, small clear vesicles.

cells, even those derived from adult animals, retain the ability to adopt a neuronal phenotype upon exposure to neurotrophic factors (Tischler *et al*. 1993). Such transdifferentiation of chromaffin cells into sympathetic neuron-like cells includes morphological, physiological and biochemical changes (Doupe *et al*. 1985; Tischler *et al*. 1993; Islas-Suarez *et al*. 1994). However, despite the wide popularity of chromaffin cells as a model for exocytosis, it is still unknown whether neuronally transdifferentiated chromaffin cells shift their pattern of exocytosis to one resembling that of a neuronal phenotype.

In the present study, we have experimentally induced a neuronal phenotype in chromaffin cell cultures and explored if a rearrangement of VGCC and secretory sites could originate a change in exocytosis pattern. To accomplish this goal, we used an astrocyte-conditioned medium (ACM) as a source of neurotrophic factors to promote transdifferentiation of chromaffin cells, and we later studied the characteristics of the exocytotic release of catecholamines. Astrocytes produce and release multiple neurotrophic factors, including nerve growth factor (NGF), basic fibroblast growth factor (bFGF), ciliary neurotrophic factor (CNTF), glial cell line-derived neurotrophic factor (GDNF) (Chiu *et al*. 1991; Rudge *et al*. 1992; Le and Esquenazi 2002), which act synergistically to induce axon and dendrite growth (Le and Esquenazi 2002). Chromaffin cells express receptors for NGF, bFGF, CNTF and GDNF (Meisinger *et al*. 1996; Suter-Crazzolara *et al*. 1996; Forander *et al*. 2000,2001; Schober *et al*. 2000). All these factors induce neurite outgrowth in chromaffin cells to varying degrees (Unsicker *et al*. 1985; Forander *et al*. 1998). Our results demonstrate that in ACM-induced transdifferentiated chromaffin cells, secretory vesicles and depolarization-induced intracellular Ca^{2+} rise are preferentially localized at neurite terminals, where the large dense-core vesicles (LDCV) exhibit a fast exocytosis mode, probably of the 'kiss-and-run' type. ACM-induced transdifferentiated chromaffin cells could constitute a suitable model, accessible to techniques that directly measure single exocytotic events that could allow us to define the mechanisms that determine the differences between exocytotic processes of neuroendocrine.

Materials and methods

Cell cultures

Bovine adrenal chromaffin cells were isolated following standard methods (Livett 1984). Briefly, cells were suspended in 1 : 1 mixture of Dulbecco's modified Eagle's medium (DMEM) and Ham's F-12 supplemented with 10% fetal calf serum, 50 IU/mL penicillin and 100 μg/mL gentamicine. Cells were plated on 12 or 25-mm-diameter glass coverslips at a density of 2.5×10^4 cells/mL. Cells were kept in a water-saturated incubator at 37°C, in a 5% CO_2/95% air atmosphere.

Astrocyte cultures were prepared from postnatal day 1 rat brain (McCarthy and De Vellis 1980). Briefly, rat cortices were digested (with 0.25% trypsin and 0.1 mg/mL DNase), trimmed and plated to 80 cm^2 culture flasks. Cells were cultured in DMEM/F12 supplemented medium, which was replaced every 2–3 days. After reaching confluence, cells were rinsed with cold medium and shaken on an orbital shaker (250 r.p.m) for 15–18 h at 37°C, to discard microglial cells by selective detachment. Under these conditions, over 90% of cells were immunoreactive for GFAP, a marker for astrocytes. ACM was obtained by conditioning DMEM/F12 medium for periods of 24–48 h.

24 h after plating, bovine chromaffin cells were incubated with ACM for 2–9 days. ACM was replaced every day. Control cells were incubated in DMEM/F12 medium, which was also replaced daily.

Immunocytochemistry

Cells were fixed in a mixture of methanol/acetone (1 : 1) for 10 min at 20°C. Proteins were blocked with 0.2% bovine serum albumin (BSA) in phosphate-buffered saline (PBS). Cells were then incubated with a monoclonal anti-dopamine β-hydroxylase (Chemicon International, Temecula, CA, USA) antibody (diluted 1 : 300 in PBS containing 0.1% BSA and 0.056% saponin) overnight at 4°C. Labelling was visualized by a FITC-conjugated antirabbit IgG antibody (Sigma-Aldrich, St Louis, MO, USA) on a confocal microscope (Zeiss, LSM-410 axiovert-100) and analysed with the NIH-J program.

Morphological Analysis

Cell morphology was assessed in cells fixed and stained against DBH. Morphological transdifferentiation was quantified by counting the number of cells that exhibit one or more neurites greater than two cell body diameters in length, and this number was expressed as a percentage of the total number in the field. The count was performed in at least four randomly selected areas of each coverslip, from a minimum of four cultures. To determine neurite elongation, cells were photographed and neurite lengths were quantified from calibrated photographs using a ruler tool from the public domain image analysis program NIH Image J.

Electron Microscopy

Chromaffin cells were cultured on sterile 40 mm diameter tissue culture dishes (Orange Scientific, Braine-l'Alleud, Belgium). The cells were fixed for 2 h at room temperature in 0.1 M cacodylate buffer (CB), pH 7.4, which contained 3% glutaraldehyde. After washing 2 h in CB, the samples were postfixed in reduced osmium (1 : 1 mixture of 2% osmium tetroxide and 3% potassium ferrocyanide) and then treated with uranyl acetate (2% aqueous solution). After fixation, the cells were dehydrated with ascending concentrations of ethanol, and finally dehydrated in propylene oxide. For inclusion, cells were pre-embedded for 1 h in a 2 : 1 mixture of propylene oxide and Eponate (Pelco, Redding, CA), then treated for 1 h in a 1 : 1 mixture of propylene oxide and Eponate, finally embedded overnight at room temperature in Eponate alone and kept at 60°C for an additional 72 h. The ultrafine sections were cut with a Reichert Ultracut E ultramicrotome, mounted on 200 mesh copper grids (Sigma) and impregnated in 4% uranyl acetate and lead citrate, pH 12. The ultrathin sections were examined under an electron microscope (Zeiss EM 900, Germany) at 50 kV, and images were recorded on EM film (Kodak Eastman, Rochester, NY, USA) at 7,500X and 23,000X magnification.

For the analysis of LDCV we included vesicles with an electron dense core and an intact vesicle membrane. For the analysis of small clear vesicles (SCV) we included only the vesicles forming clusters. The diameter of secretory vesicles was determined by measuring the vesicular perimeter using the public domain Image J software (NIH, Bethesda, MD, USA). Corrected vesicle diameter was calculated using a previously published algorithm (Parsons *et al*. 1995). This algorithm is dependent on section thickness and the empirical measured vesicle diameter. Section thickness was estimated to be 70 nm based on the silver interference color of the sections (Sakai 1980).

Intracellular Ca^{2+} imaging experiments

Ca^{2+} imaging experiments were performed in Fluo-4 loaded cells, as described previously (Mendoza *et al*. 2003). Chromaffin cells cultured on glass coverslips were loaded with Fluo-4 AM (5 μM in 0.1% pluronic acid) at 20°C for 30 min and later washed with a Krebs-HEPES buffer solution (in mM: 140 NaCl, 5 KCl, 2 $MgCl_2$, 2.5 $CaCl_2$, HEPES-NaOH and 10 glucose; pH = 7.4). Depolarization was achieved by KCl using a pressure-driven microejection system. The stimulus pipette, tip diameter of *ca*. 1 μm, was filled with 70 mM KCl and positioned at 10–15 μm from the cell. Images were recorded from the central plane of the cells with a Sensicam® QE cooled digital camera (Cooke Corporation, Romulus, MI, USA) attached to a Nikon Eclipse TE-2000 inverted microscope (objective 40x) at intervals of 250 ms, and analyzed with the NIH Image program. All fluorescence data are expressed as the increase in fluorescence divided by baseline fluorescence (ΔF/F).

Amperometric Detection of Exocytosis

Carbon fibers of 8-μm radius (Thornel P-55; Amoco Corp., Greenville SC, USA) were used to make the microelectrodes (Kawagoe *et al*. 1993). Electrochemical recordings were performed using an Axopatch 1C (Axon Instruments, Union City, CA, USA). Cells were placed in a perfusion chamber positioned on the stage of an inverted microscope and washed in Krebs-HEPES buffer solution. Amperometric measurements were performed with a carbon fiber microelectrode gently touching the cell membrane. Catecholamine release was stimulated by 5-s pressure ejection of 70 mM K^+ from a micropipette positioned at 10–15 μm from the cell. For experiments in cells loaded with EGTA, cells were incubated with 20 μM EGTA-AM (Molecular Probes, Eugene, Oregon, USA) during 45 min. Then, cells were washed in Krebs-HEPES buffer solution and depolarized with a 70 mM K^+ pulse.

Amperometric records were low-pass filtered at 1 KHz, sampled at 5 KHz, and collected using PClamp 8.1 (Axon Instruments). To analyze the exocytotic events, a series of kinetic parameters were extracted from each spike. Data analysis was carried out using locally written macros for IGOR (Wavemetrics, Lake Oswego, OR, USA). These macros allowed the automatic digital filtering, secretory spike identification, and data analysis (Segura *et al*. 2000). All the above macros and their user instructions can be downloaded free from the following web address: http://webpages.ull.es/users/rborges/.

Statistics

Normalized results were expressed as means ± SEM. Amperometric spike data were grouped by individual cells, thus data correspond to means ± SEM of the cell median for each spike parameter, where 'n' refers to the number of cells. Statistical comparisons were performed utilizing the non-parametric U-Mann–Whitney test.

Results

ACM promotes neurite extension in chromaffin cells

In the presence of ACM, chromaffin cells from adult bovine adrenal medulla extend one or more neurite processes (Fig. 1a). Fifty percent and 79 ± 3.0% of bovine chromaffin cells exhibited neurites after 4 and 7 days under ACM treatment, while 13 ± 5% and 53 ± 4% of the chromaffin cells had neurites in control cultures during the same periods of time (Fig. 1b). ACM treatment also significantly enhanced neurite elongation (Fig. 1c). The length of neurite processes reached 43 ± 2 μm ($n = 72$) and 145.6 ± 11 μm ($n = 53$), after 4 and 7 days of exposure to ACM ($p < 0.0005$ compared with the length of neurites of cells in control conditions). The analysis of the distribution of the vesicular enzyme dopamine β-hydroxylase (DBH) indicated that the secretory vesicles were preferentially distributed in the neurite terminals; the DBH immunoreactivity ratio of neurite terminal/soma was 3.6 ± 0.4 fold ($n = 60$) for ACM-treated cells and 2.7 ± 0.2 fold ($n = 50$) for cells that extend neurite in control medium.

ACM-treated cells exhibited amperometric signals mainly in the neurite terminals

By using amperometry we examined the frequency of exocytotic events at neurites and somas of cells cultured in the absence and in the presence of ACM for short (2–4 days) and long (7–9 days) periods of time. Exocytosis was stimulated by the application of a high K^+ pulse. As shown in Fig. 2(a), ACM-treated cells with a neuronal phenotype exhibited amperometric signals mainly in the neurite terminals, while the exocytotic events in the corresponding somas were significantly more scarce ($p < 0.0005$). The frequency of exocytotic events in the neurite terminals of cells exposed to ACM for both short- and long-time periods was similar to that observed in cells kept in control medium for 2–4 days. On the other hand, spherical and neuron-like spherical cells maintained for longer periods in the control medium exhibited a low frequency of exocytotic events (Fig. 2a). Normally, chromaffin cell cultures have a lifetime of no more than one week, thus the scarce exocytosis of cells maintained for long-time periods in control medium could be a consequence of the un-healthy condition of these cells. Conversely, the good response observed in neurite terminals of ACM-treated cells could be a consequence of the reported protective properties of the astrocyte-released factors (Cui *et al*. 2001).

Figure 2(b–d) show amperometric recordings obtained from a spherical cell in control medium during 3 days, and from neurites of chromaffin cells exposed to ACM for short-

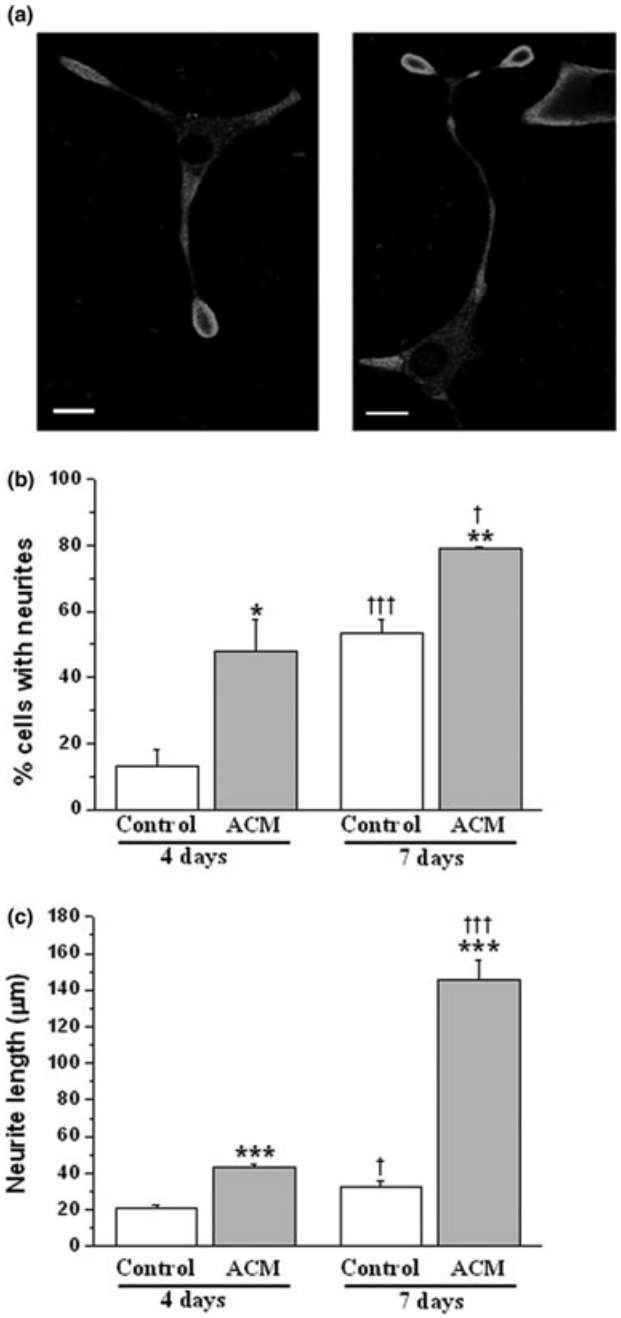

Fig. 1 ACM induced neurite outgrowth in bovine chromaffin cells. 24 h after plating, chromaffin cells were kept in control media (white bars) or exposed to ACM (grey bars) for 4 or 7 days. (a) Representative confocal images of chromaffin cells exposed to ACM and immunostained for DBH. Z-axis resolution was 0.8 μm. Scale bars = 20 μm. (b) Percentage of cells with neurite processes (means from 5 different cultures). (c) Neurite lengths (means from 72 and 53 cells). Data are means ± SEM $^{*}p < 0.05$, $^{**}p < 0.005$, $^{***}p < 0.0005$ compared to control cells; $\dagger p < 0.05$, $\dagger\dagger\dagger p < 0.0005$ compared with cells kept during 4 days in control medium or ACM.

or long-time period. Note that the individual spikes shown in right panels exhibited different characteristics for each experimental condition.

Neurite terminals of chromaffin cells exposed to ACM for 7–9 days exhibit fast exocytosis events

The properties of the amperometric spikes of cells in the control medium or exposed to ACM for short or long time periods are compared in Table 1. The amperometric spikes recorded in the neurites of ACM-treated cells, for either short or long time periods, had quantal size (Q) that was 25–35% smaller than that of chromaffin cells maintained in control medium ($p < 0.05$). Interestingly, the exocytotic events in neurite terminals of long-term ACM-treated cells were drastically accelerated; the mean of half width ($t_{1/2}$) was 40% shorter than that recorded in either control cells or short-term ACM-treated cells (Table 1). The rapid exocytosis was not a consequence of time in culture, since cells, with spherical or neuronal phenotype, in the control conditions for long-time periods exhibited $t_{1/2}$ values larger than those of neurite terminals of long-term ACM-treated cells (Table 1). The $t_{1/2}$-values of somas of long-term ACM-treated cells ($t_{1/2} = 11.1 \pm 1.2$ s, 27 cells) were also significantly larger than those of neurite terminals of long-term ACM-treated cells ($p < 0.05$).

We discount the possibility that the kinetic acceleration observed in neurite terminals of long-term ACM-treated cells was a consequence of a different morphology, since the kinetic parameters of neurites of long-term ACM-treated cells were significantly different from those observed in neurites of either short-term ACM-treated or age-matched control cells (Table 1). To insure that the morphology does not affect amperometric spike parameters, we simulated amperometric spikes using Monte Carlo methods (Haller *et al.* 1998), and compared the spike parameters in a spherical cell with a diameter of 15 μm and in an elliptical neurite terminal with a width of 7.5 μm. These simulations demonstrated that the $t_{1/2}$-values could be only 2.5% faster in an elliptical neurite terminal (Please see Fig. 1 in supplementary information).

To determine whether the $t_{1/2}$ reduction in long-term ACM-treated cells was due to the ascending or the decay phases, other kinetic parameters of the amperometric spikes were analysed. Table 1 shows the values of the ascending slope (m), and the decay time constants, τ and τ'. The ascending phase has been related with fusion pore expansion (Schroeder *et al.* 1996; Alés *et al.* 2005). As shown in Table 1, the ascending slope was significantly faster in the neurite terminals of long-term ACM-treated cells. The spike decay phase, which fits with a double exponential in chromaffin cells (Machado *et al.* 2000), has been related with either the fusion pore closure (Elhamdani *et al.* 2001; Graham *et al.* 2002) or catecholamine dissociation from the intravesicular matrix (Schroeder *et al.* 1996). The amperometric spikes observed in

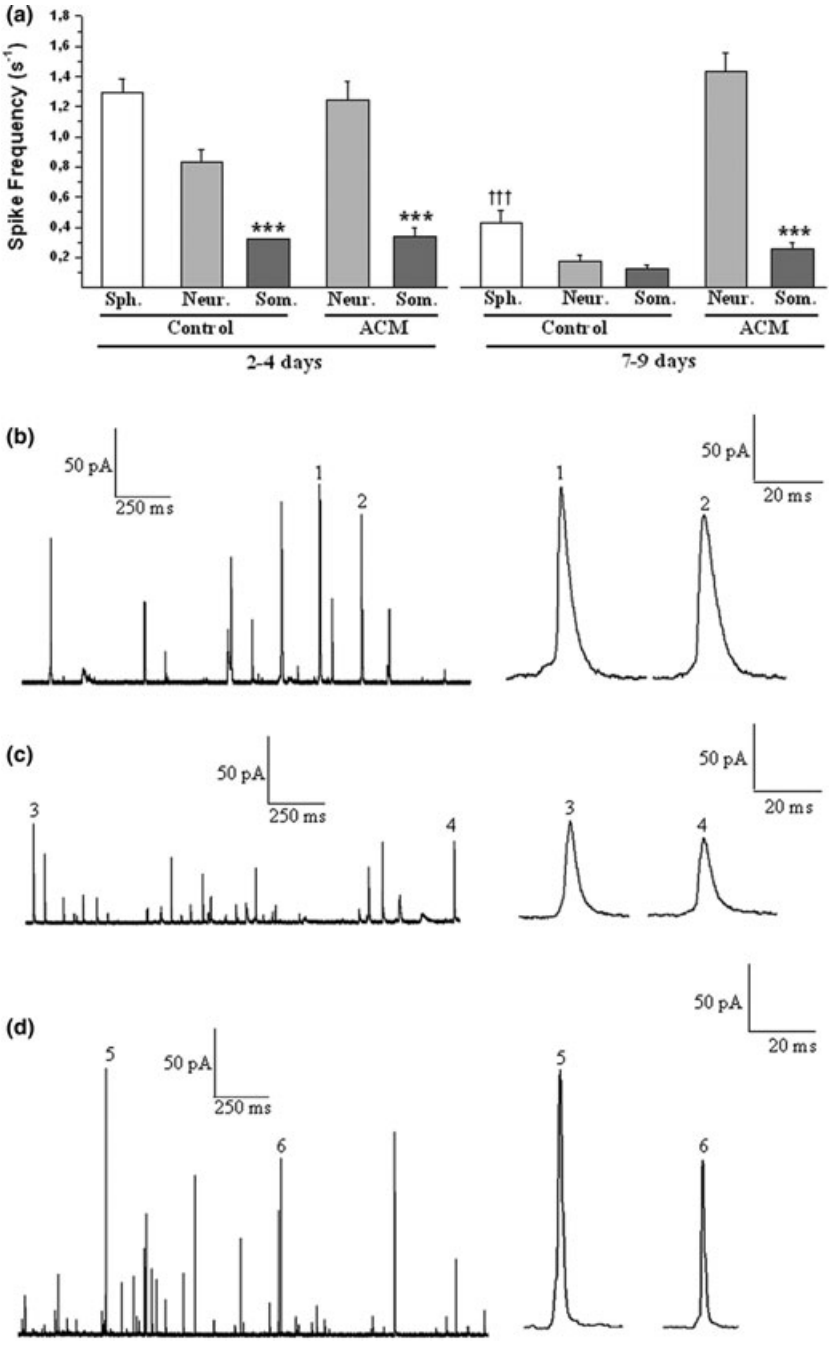

Fig. 2 ACM-treated cells exhibited amperometric signals mainly in neurite terminals. Amperometric spikes were induced with a high K^+ pulse. (a) Mean values for spike frequency in spherical cells (Sph.) or neurite terminals (Neur.) and somas (Som.) of cells kept in control condition (Control) or exposed to ACM for 2–4 or 7–9 days. Data are means ± SEM of cell median (24–30 cells from 3 to 5 different cultures). ***$p < 0.0005$ compared with neurite terminals; †††$p < 0.0005$ compared with spherical cells kept in control medium for 2–4 days. Amperometric recordings from a spherical chromaffin cell maintained in control condition during 3 days (b), or from neurite terminals of chromaffin cells exposed to ACM for 3 days (c) or 8 days (d). The right panels show representative spikes taken from the recordings of the left panels, as indicated by the corresponding numbering.

neurites of ACM-treated cells also fit with a double exponential, but τ and τ' values were also significantly faster in the neurite terminals of long-term ACM-treated cells ($p < 0.05$) compared with either control cells or neurites of cells exposed for short-time periods to ACM.

Long-term treatment with ACM modifies the fusion pore stability

The current that precedes the amperometric spike, also called 'foot signal', has been related to the slow release of catecholamines through a narrow fusion pore (Chow *et al.* 1992). The duration of the foot signal indicates the stability of the fusion pore, while the current amplitude of the foot has been related to the flux of neurotransmitters through the pore (Mosharov & Sulzer 2005). Therefore, we compared the duration and the current amplitude of the foot signals of amperometric spikes from neurites of cells exposed to ACM with those from spherical control cells. Figure 3 shows representative amperometric spikes with foot signals from control cells and from neurite terminals of cells exposed to

Table 1 Properties of amperometric spikes of neurite terminals of chromaffin cells exposed to ACM

	Q (pC)	$t_{1/2}$ (ms)	m (nA/s)	τ (ms)	τ' (ms)
Control Condition					
2–4 days					
Spherical cells	0.74 ± 0.07	9.2 ± 0.75	31.7 ± 3.7	4.7 ± 0.4	9.1 ± 0.8
Neurite terminals	0.59 ± 0.08	10.6 ± 0.9	17.5 ± 3.0	5.7 ± 0.7	10.2 ± 1.0
7–9 days					
Spherical cells	0.69 ± 0.11	9.1 ± 1.1	20.1 ± 2.6	4.9 ± 0.8	12.5 ± 2.2
Neurite terminals	0.92 ± 0.13	9.4 ± 1.3	24.5 ± 4.3	4.6 ± 0.6	10.1 ± 1.3
ACM					
2–4 days					
Neurite terminals	0.56 ± 0.05[b]	9.0 ± 0.68	25.7 ± 2.6	4.6 ± 0.3	9.1 ± 0.8
7–9 days					
Neurite terminals	0.49 ± 0.06[a,b,c]	5.6 ± 0.49[a,b,c]	50.2 ± 6.8[a,b,c]	2.8 ± 0.3[b,b,c]	5.3 ± 0.5[a,b,c]

Q is the integrated area under the spike trace that indicates the total catecholamines released during an exocytotic event; $t_{1/2}$ is the spike width at its half height; m is the ascending slope between 25 and 75% of spike ascent, τ and τ' are the time constants of the decay phase. Data are means ± SEM. of cell median for each spike parameters (24–30 cells from 3 to 5 different cultures). [a]$p < 0.05$ compared with spherical control cells; [b]$p < 0.05$ compared with neurites of control cells; [c]$p < 0.005$ compared with cells exposed to ACM for 2–3 days.

ACM. The percentage of amperometric spikes with foot signals was similar for control chromaffin cells and neurites of cells exposed to ACM (Fig. 3b). However, the duration of the foot at neurites of ACM-treated cells was significantly shorter than in cells in control medium, indicating that the treatment with ACM modifies the stability of the fusion pore. A short-term exposure to ACM was sufficient to produce this effect. On the other hand, the current amplitude of foot signals was similar for spherical cells in control medium and neurites of cells exposed to ACM (Fig. 3b).

Chromaffin cells exposed to ACM contain both large dense-core and small clear vesicles

SCV forming clusters have been observed in neurites of rat chromaffin cells exposed for a long-time period to NGF (Doupe *et al*. 1985). To determine whether the smaller quantal size of ACM-treated cells was a consequence of a decrease in vesicular size, we examined ACM treated and non-treated cells under the electron microscope.

Figure 4 shows electron micrographs of chromaffin cells cultured on control medium and from cultures exposed to ACM for one week. These electron micrographs reveal the presence of LDCV in somas and neurites of ACM-treated cells. However, the presence of SCV in neurite terminals is particularly interesting (see arrow in Fig. 4d). The mean of SCV diameters was approximately 40% of that of LDCV of control cells (Fig. 4e). The size of LDCV of cells exposed to ACM was not significantly different to those of control cells (Fig. 4e). Frequency distributions of vesicle diameters from neurites of cells exposed to ACM are shown Fig. 4(f). The vesicle diameter was fitted to two Gaussian curves ($R = 0.98$), with peaks at 269 nm and 116 nm.

The rapid exocytosis events observed in neurites of cells exposed to ACM correspond to LDCV exocytosis

As the cubic root of the quantal size ($Q^{1/3}$) has been related to the vesicle diameter and electron micrographs of the neurite terminals revealed the presence of both SCV and LDCV in neurites (Fig. 4), we used this parameter to investigate whether the rapid exocytosis events correspond to SCV or LDCV.

As shown in Fig. 5(a), $Q^{1/3}$ was significantly smaller for the spikes recorded from neurites of cells exposed to ACM for both short- and long-time periods ($p < 0.05$) than those for untreated cells. The distribution of $Q^{1/3}$-values of spikes from control cells was fitted to a Gaussian curve ($R = 0.96$), with a peak at 0.77 $pC^{1/3}$. For neurite terminals of cells exposed to ACM for both short- and long-time periods, the distribution of $Q^{1/3}$-values was also fitted to a Gaussian curve ($R = 0.97$ and 0.98), with peaks at 0.71 and 0.68 $pC^{1/3}$, respectively (Fig. 5b). Figure 5(c) show the overlap of the Gaussian curves for the $Q^{1/3}$ of spikes obtained from cells cultured under control conditions and from spikes from neurites of long-term ACM-treated cells. A general leftward shift to lower values is observed for cells exposed during 7–9 days to ACM. But, it is not observed an additional population corresponding to SCV, whose diameters were 2.5 times smaller than that of LDCV of control cells.

Neurite terminals of cells exposed to ACM exhibit higher intracellular Ca^{2+} signals than somas

We also investigated if astrocyte-released factors change the distribution pattern of the intracellular Ca^{2+} responses to a depolarizing stimulus in chromaffin cells. Thus, we compared the distribution of depolarization-induced Ca^{2+} signals in cells that extend neurites when cultured under control

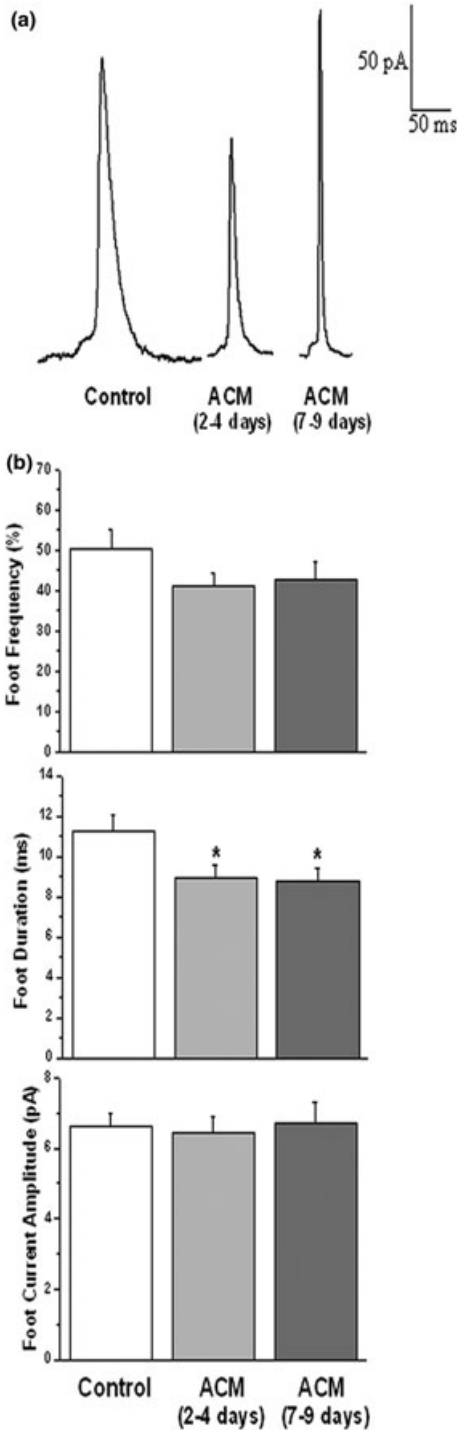

Fig. 3 Exposure to ACM modifies fusion pore stability. (a) Representative amperometric spikes with foot signals from spherical control cells (2–4 days) and neurite terminals of cells exposed to ACM. (b) Foot frequency (percentage of spikes with foot per cell), duration and current amplitude of chromaffin cells in control medium or from neurites of cells exposed to ACM for 2–4 days or 7–9 days. Data are means ± SEM of cell median for each foot parameters (26–30 cells from 3 to 5 different cultures). *$p < 0.05$ compared to chromaffin cells in the control medium.

conditions, with cells that extended neurites in the presence of ACM during short (2–4 days) and long (7–9 days) time periods.

Figure 6a and b shows a temporal sequence of a representative fluorescence change ($\Delta F/F_0$) in chromaffin cells exposed to ACM for 3 and 8 days, respectively. Note the higher fluorescence in the neurite terminals as compared with the somas.

As shown in Fig. 6(c) the fluorescence ratio of neurite terminal/soma for cells exposed to ACM for short- or long-time periods was 2.0 ± 0.4 ($n = 28$) and 1.6 ± 0.2 ($n = 32$). Both values were significantly larger than those obtained in cells kept in the control condition ($p < 0.05$). These results suggest that ACM promotes a preferential distribution of intracellular Ca^{2+} responses at the neurite terminal.

The secretory vesicles and VGCC are coupled more closely in the neurite terminals of ACM-treated cells

Calcium chelators have been widely used to investigate the Ca^{2+} dependence of fast neurotransmitter release (Atluri and Regehr 1996; Borst and Sakmann 1996; Beaumont *et al.* 2005). In particular, the slow acting Ca^{2+} chelator EGTA has been helpful to infer the spatiotemporal dependence of Ca^{2+}-dependent phenomena (Neher 1998). Consequently, we performed experiments in cells loaded with EGTA to see whether secretory vesicles and VGCC are coupled more closely in the neurite-terminal of ACM-treated cells than in the spherical chromaffin cells.

For control cells, the number of amperometric spikes induced by depolarisation decreased by 84% when the intracellular Ca^{2+} was buffered with EGTA (Fig. 7a), suggesting that only a small number of vesicles are tightly coupled to VGCC. In short-term ACM-treated cells, the spike frequency was also drastically reduced when the cells were loaded with EGTA. However, in cells exposed to ACM for longer-time periods, the number of amperometric spikes decreased by only 30% when the intracellular Ca^{2+} was buffered with EGTA (Fig. 7a). These data suggest that a larger number of secretory vesicles are tightly coupled to VGCC in the neurite terminals of long-term ACM-treated cells, as compared with spherical control cells or neurites of short-term ACM-treated cells.

Both in control cells and ACM-treated cells, half width values were not significantly affected when the intracellular Ca^{2+} was buffered with EGTA (Fig. 7b). However, quantal size was significantly larger when the intracellular Ca^{2+} was buffered with EGTA in both cells kept under control conditions and exposed to ACM for short-time periods (Fig. 7c). Quantal size was not modified by EGTA in long-term ACM-treated cells.

When the fast Ca^{2+} chelator BAPTA was used to buffer the intracellular Ca^{2+} of cells cultured in the presence or in the absence of ACM, none or only one spike was observed in the amperometric recordings (6–12 cells).

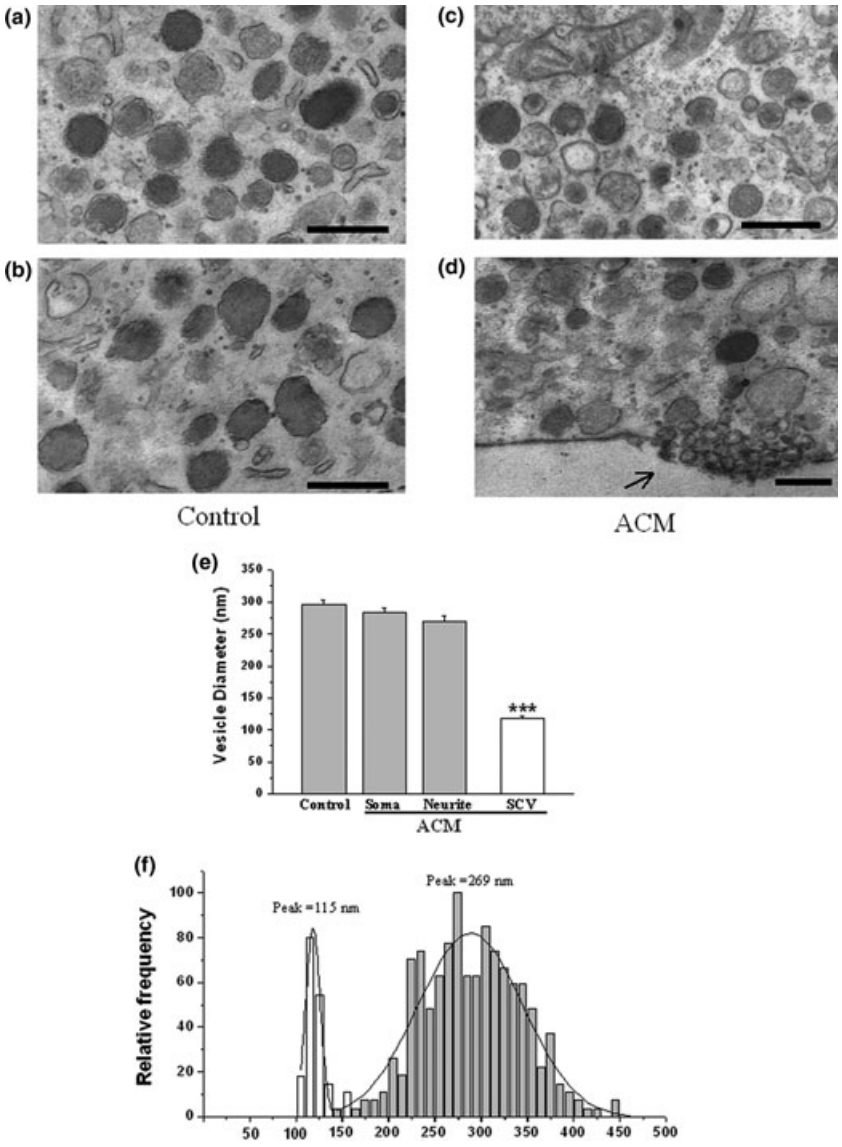

Fig. 4 Chromaffin cells exposed to ACM have both LDCV and SCV. Electron micrographs of chromaffin cells in control medium (a and b) or exposed to ACM (c and d). Micrographs c and d correspond to the soma and a neurite of a cell exposed to ACM. The arrow shows the cluster of SCV. Scale bar = 500 nm. (e) Mean values for vesicle diameters of LDCV (grey bars) and SCV (white bar) from chromaffin cells in control medium (control) or somas and neurites of chromaffin cells exposed to ACM. Data are means ± SEM of cell median from 3 cells. ***$p < 0.0005$ compared with LDCV diameters. (f) Frequency distribution of vesicle diameters of LDCV (gray bars) and SCV (white bars) from neurites of cells exposed to ACM.

Discussion

The present results demonstrated that astrocyte-released factors induced neurite extensions in bovine chromaffin cells, and promoted a preferential distribution of secretory vesicles and depolarization-induced intracellular Ca^{2+} rise at neurite terminals (Figs 1 and 6). Interestingly, important changes occur in exocytosis after a long-term exposure to astrocyte-released factors.

After 4 weeks in culture in the presence of both NGF and a heart cell conditioned medium, rat chromaffin exhibit morphology indistinguishable from sympathetic neurons (Doupe *et al*. 1985). Those neuronal-type chromaffin cells displayed SCV and synthesized and stored acetylcholine. Although we did not expose the bovine chromaffin cells to ACM for more than 9 days, we observed some clusters of SCV. However, the comparison of $Q^{1/3}$ and vesicle diameter distributions indicates that the exocytotic events observed in neurites of cells exposed to ACM correspond to the exocytosis of LDCV, and not of SCV. It is plausible, however, that the SCV population is still undetectable by amperometry in our experimental conditions. On the other hand, SCV could likely correspond to vesicles that store acetylcholine, as previously described for PC12 cells (Bauerfeind *et al*. 1993). The exocytosis from acetylcholine vesicle is undetectable by conventional amperometry (Xin and Wightman 1997); therefore it is necessary to analyze the SCV contents in cells exposed to ACM to confirm that hypothesis.

We observed that different steps of LDCV exocytosis were significantly modified when chromaffin cells adopted a neuronal phenotype in the presence of ACM. The foot duration of cells exposed to ACM was significantly smaller than that of control cells, suggesting that the exposure to

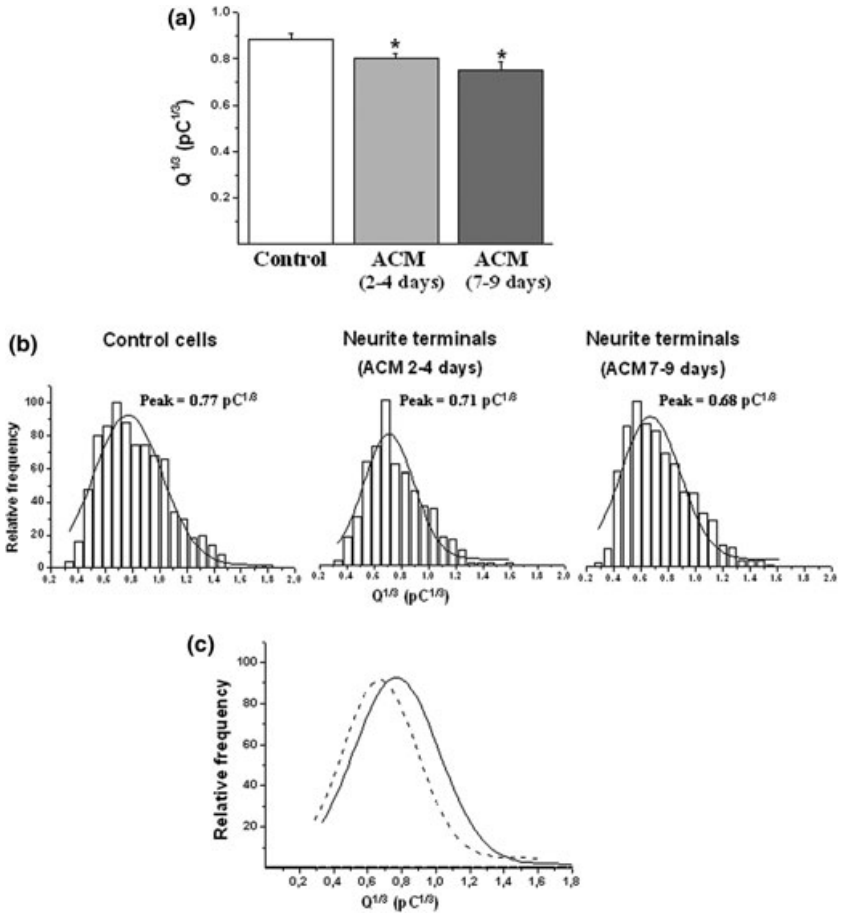

Fig. 5 Exocytotic events at neurites of ACM-treated cells correspond to LDCV exocytosis. (a) Mean values for $Q^{1/3}$ (cubic root of the quantal size). Data are means ± SEM of cell median for each spike parameter (26–30 cells from 3 to 5 different cultures). *$p < 0.05$ compared with chromaffin cells in the control condition. (b) Frequency distribution of $Q^{1/3}$-values from chromaffin cells in control medium (566 spikes) or from neurites of cells exposed to ACM for 2–4 days (470 spikes) or 7–9 days (730 spikes). (c) Overlap of the Gaussian curves of the $Q^{1/3}$ from control cells (solid line) and neurite terminals of cells exposed to ACM for 7–9 days (dashed line).

astrocyte-released factors change the fusion pore stability. A short-term exposure (2–4 days) to ACM seems to be enough to produce such effect (Fig. 3). The composition of the fusion pore remains to be fully elucidated (Han *et al*. 2004). However, the SNARE protein synaptobrevin II (Borisovska *et al*. 2005) and the calcium sensor proteins synaptotagmin I and IV (Wang *et al*. 2001) can determine the fusion pore stability; while synaptotagmin I prolongs the time from fusion pore opening to expansion, synaptotagmin IV shortens this time. Neurotrophic factors produced by astrocytes modify the expression and/or distribution patterns of some of those proteins that interact with the fusion pore; for instance, NGF sorts synaptotagmin IV, which is localized on the Golgi membrane in undifferentiated PC12 cells, to LDCV at neurite terminals (Fukuda *et al*. 2003). Bovine chromaffin cells express synaptotagmin I (Yoo *et al*. 2005), however, other synaptotagmin isoforms have not been identified yet. Therefore, the study of the expression of the different synaptotagmin isoforms could help to a better understanding of the molecular mechanisms that drive exocytosis in chromaffin cells.

Another interesting finding of our experiments was the drastic acceleration of the exocytotic events observed in the long term ACM-treated cells. This acceleration was observed in both the ascent and decay phases of the amperometric spikes. The spike ascent phase is determined by the fusion pore expansion rate (Schroeder *et al*. 1996), which reportedly depends on intracellular Ca^{2+} concentrations (Hartmann and Lindau, 1995; Scepek *et al*. 1998).

ACM promoted a preferential distribution of secretory vesicles and depolarization-induced intracellular Ca^{2+} rise in neurite terminals (Figs 1 and 6). Chromaffin cells that extend neurites in control medium also accumulate secretory vesicles at neurite terminals (Gil *et al*. 2001). However, in those cells intracellular Ca^{2+} responses to depolarization were not preferentially distributed in the neurite terminal, like it is observed in ACM-treated cells (Fig. 6c). This pattern of intracellular Ca^{2+} distribution, which could be a consequence of a redistribution of VGCC and/or modification in the mechanisms that regulate the intracellular Ca^{2+} homeostasis (Jiménez and Hernández-Cruz 2001), was observed in cells exposed to ACM for either short- or long-time periods. Therefore, additional changes should occur after a long-term exposure to ACM that allows shifting the exocytosis kinetics. The experiments performed in EGTA-loaded cells suggest a change in the coupling between secretory vesicles and

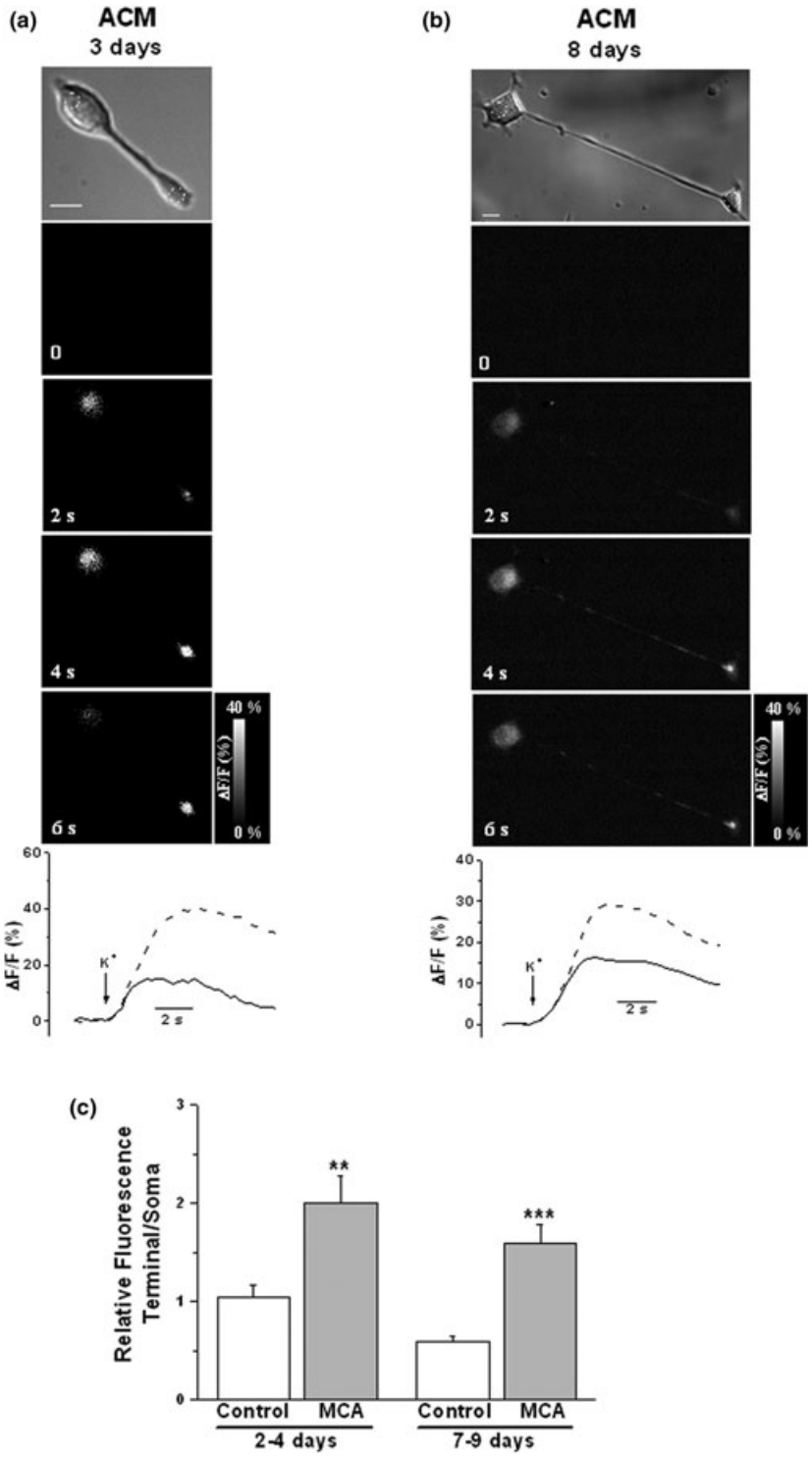

Fig. 6 Neurite terminals of cells exposed to ACM exhibit higher intracellular Ca^{2+} signals than somas. Fluo-4-loaded chromaffin cells were stimulated with a 5 s pulse of 70 mM K^+. (a–b): The top panels show cells exposed to ACM for 3 (a) and 8 days (b) visualized with differential interference contrast. The regions of interest are indicated with white circles. Scale bars = 20 μm. Middle panels show Ca^{2+} images before (0) and 2, 4 and 6 s after the high K^+ pulse. The grey-scale bar is expressed as $\Delta F/F_0$ (%). Images were collected at 4.0 Hz. The bottom panel shows temporal plots of $\Delta F/F_0$ in soma (solid line) and neurite terminal (dashed line) from each cell. The arrow shows the high K^+ pulse application. c: Data are means ± SEM of fluorescence ratio of neurite terminal/soma for cells that spontaneously emitted neurites in the control condition (Control) or cells exposed to ACM for 2–4 or 7–9 days (26–30 cells from 3 to 5 different cultures). $^{**}p < 0.005$, $^{***}p < 0.0005$ compared with cells that spontaneously emitted neurites in control condition.

VGCC during the transdifferentiation of chromaffin cells. The buffering of the intracellular Ca^{2+} with EGTA reduces the area of the Ca^{2+} microdomains; in consequence vesicles that are more distant from the VGCC do not sense enough Ca^{2+} to trigger the exocytosis (Neher 1998). In this regard, the experiments in EGTA-loaded cells suggest that a larger number of secretory vesicles are tightly coupled to VGCC in the neurite terminals of cells exposed for long-time periods to ACM, in comparison to either control chromaffin cells or short-term ACM-treated cells (Fig. 7a). N and P/Q calcium channels bind SNARE proteins through a synaptic protein interaction (synprint) site, which contribute to the tight

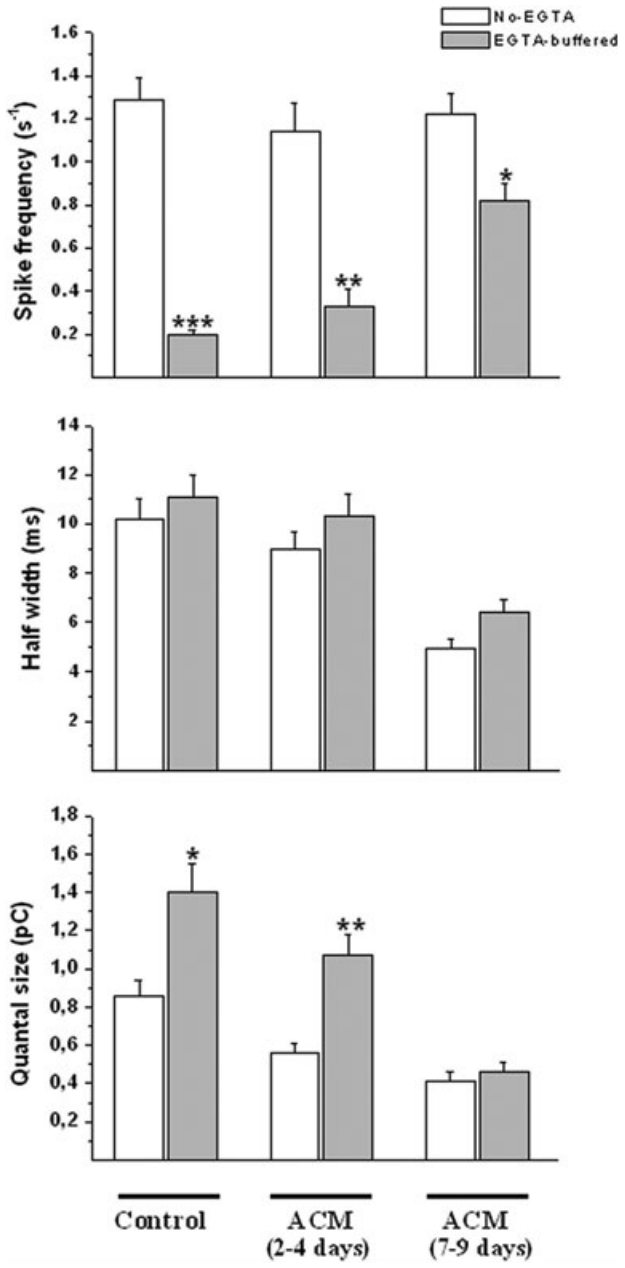

Fig. 7 ACM promote better coupling between secretory vesicles and VGCC. Chromaffin cells in control condition (Control) or exposed to ACM for 2–4 days or 7–9 days, were loaded with 20 μM EGTA-AM during 45 min. Then, cells were washed in Krebs-HEPES buffer solution and depolarized with a high K^+ pulse. Data are means ± SEM of cell median (20–32 cells) for spike frequency, half width and quantal size. $^*p < 0.05$, $^{**}p < 0.005$, $^{***}p < 0.0005$ compared with cells non-loaded with EGTA.

coupling between those types of VGCC with proteins of the exocytotic machinery (Catterall 1999). In a recent report, Andres-Mateos *et al*. (2005) have demonstrated a dynamic association of P/Q calcium channels with SNAP-25 during the transdifferentiation of chromaffin cells. Those authors observed that P/Q channels and SNAP-25 first migrate separately to the developing neurite, but later they colocalize at the terminals of mature neurites. Therefore, the rearrangement of the different types of VGCC and their association to SNARE proteins that probably occur during the transdifferentiation could determine the shift in exocytotic kinetics.

The spike quantal size was also reduced in neurite terminals of ACM-treated cells, an effect that was found to be time-dependent (Table 1). A reduction in the spike quantal size has been related with 'kiss-and-run' events in chromaffin cells (Archer *et al*. 2002; Graham *et al*. 2002; Chen *et al*. 2005). 'Kiss-and-run' events are characterized by transient fusion of vesicles, demonstrated as brief flickers in capacitance measurement (Albillos *et al*. 1997). By using patch-amperometry, two types of 'kiss-and-run' events have been described in chromaffin cells: 'stand-alone foot' and 'fast kiss-and-run'. 'Stand-alone foot' events occur with partial catecholamine release in a foot signal-like form, while fast 'kiss-and-run' events occur with catecholamine released in a spike-like form (Alés *et al*. 1999). High Ca^{2+} concentrations promote 'fast kiss-and-run' events in chromaffin cells (Alés *et al*. 1999). Then, 'fast kiss-and-run' could be the most predominate exocytosis mode in neurites of ACM-treated chromaffin cells. However, we acknowledge that patch-amperometry experiments are necessary to fully demonstrate this hypothesis (Alés *et al*. 1999).

The many changes that occur in the exocytosis with phenotype conversion indicate that transdifferentiated chromaffin cells shift their pattern of exocytosis to one more appropriate for the neuronal phenotype. The colocalization of VGCC and proteins of the exocytotic machinery at active zones of neurites seems to be important for those changes. However, additional studies are required to explore whether proteins of the exocytotic machinery change during the transdifferentiation of chromaffin cells.

Acknowledgements

This work was supported by Fondecyt 1020812 and 7020812, and DIPUV 37– 2004. We thank Dr Guillermo Alvarez de Toledo and Dr Humberto Viveros for their worthy comments; Dr Guillermo Alvarez de Toledo and Carlos Fernández Peruchena for their invaluable help in using Monte Carlo simulation and David Memmott for reviewing the manuscript. JM and IGM are students from Instituto de Química, Pontificia Universidad Católica de Valparaíso. EA is supported by Ramón y Cajal Programme (Spain).

Supplementary material

The following material is available for this article online

This material is available as part of the online article from http://www.blackwell-synergy.com

References

Albillos A., Dernick G., Horstmann H., Almers W., Alvarez de Toledo G. and Lindau M. (1997) The exocytotic event in chromaffin cells revealed by patch amperometry. *Nature* **389**, 509–512.

Alés E., Tabares L., Poyato J. M., Valero V., Lindau M. and Alvarez de Toledo G. (1999) High calcium concentrations shift the mode of exocytosis to the kiss-and-run mechanism. *Nat. Cell. Biol.* **1**, 40–44.

Alés E., Ñeco P., Gutierrez L. M. and Alvarez de Toledo G. (2005) Regulation of the fusion pore expansion during exocitosis by myosin II. *J. Physiol. Biochem.* **61**, 96.

Andres-Mateos E., Renart J., Cruces J., Solis-Garrido L. M., Serantes R., de Lucas-Cerrillo A. M., Aldea M., Garcia A. G. and Montiel C. (2005) Dynamic association of the Ca^{2+} channel alpha1A subunit and SNAP-25 in round or neurite-emitting chromaffin cells. *Eur. J. Neurosci.* **22**, 2187–2198.

Archer D. A., Graham M. E. and Burgoyne R. D. (2002) Complexin regulates the closure of the fusion pore during regulated vesicle exocytosis. *J. Biol. Chem.* **277**, 18249–18252.

Atluri P. P. and Regehr W. G. (1996) Determinants of the time course of facilitation at the granule cell to Purkinje cell synapse. *J. Neurosci.* **16**, 5661–5671.

Bauerfeind R., Regnier-Vigouroux A., Flatmark T. and Huttner W. B. (1993) Selective storage of acetylcholine, but not catecholamines, in neuroendocrine synaptic-like microvesicles of early endosomal origin. *Neuron* **11**, 105–121.

Beaumont V., Llobet A. and Lagnado L. (2005) Expansion of calcium microdomains regulates fast exocytosis at a ribbon synapse. *Proc. Natl Acad. Sci. USA* **102**, 10 700–10 705.

Borisovska M., Zhao Y., Tsytsyura Y., Glyvuk N., Takamori S., Matti U., Rettig J., Sudhof T. and Bruns D. (2005) v-SNAREs control exocytosis of vesicles from priming to fusion. *EMBO J.* **24**, 2114–2126.

Borst J. G. and Sakmann B. (1996) Calcium influx and transmitter release in a fast CNS synapse. *Nature* **383**, 431–434.

Burgoyne R. D. and Morgan A. (1998) Calcium sensors in regulated exocytosis. *Cell Calcium* **24**, 367–376.

Catterall W. A. (1999) Interactions of presynaptic Ca2+ channels and snare proteins in neurotransmitter release. *Ann. N. Y. Acad. Sci.* **868**, 144–159.

Chen X. K., Wang L. C., Zhou Y., Cai Q., Prakriya M., Duan K. L., Sheng Z. H., Lingle C. and Zhou Z. (2005) Activation of GPCRs modulates quantal size in chromaffin cells through $G_{\beta\gamma}$ and PKC. *Nat. Neurosci.* **8**, 1160–1168.

Chiu A. Y., Espinosa de los Monteros A., Cole R. A., Loera S. and de Vellis J. (1991) Laminin and s-laminin are produced and released by astrocytes, Schwann cells, and schwannomas in culture. *Glia* **4**, 11–24.

Chow R. H., von Ruden L. and Neher E. (1992) Delay in vesicle fusion revealed by electrochemical monitoring of single secretory events in adrenal chromaffin cells. *Nature* **356**, 60–63.

Cui W., Allen N. D., Skynner M., Gusterson B. and Clark A. J. (2001) Inducible ablation of astrocytes shows that these cells are required for neuronal survival in the adult brain. *Glia* **34**, 272–282.

Doupe A. J., Landis S. C. and Patterson P. H. (1985) Environmental influences in the development of neural crest derivatives: glucocorticoids, growth factors, and chromaffin cell plasticity. *J. Neurosci.* **5**, 2119–2142.

Elhamdani A., Palfrey H. C. and Artalejo C. R. (2001) Quantal size is dependent on stimulation frequency and calcium entry in calf chromaffin cells. *Neuron* **31**, 819–830.

Forander P., Brene S. and Stromberg I. (2000) Expression and regulation of CNTF receptor-alpha in the in situ and in oculo grafted adult rat adrenal medulla. *Neuroreport* **11**, 593–597.

Forander P., Broberger C. and Stromberg I. (2001) Glial-cell-line-derived neurotrophic factor induces nerve fibre formation in primary cultures of adrenal chromaffin cells. *Cell Tissue Res.* **305**, 43–45.

Forander P., Hoffer B. and Stromberg I. (1998) Nerve fiber formation and catecholamine content in adult rat adrenal medullary transplants after treatment with NGF, NT-3, NT-4/5, bFGF, CNTF, and GDNF. *Cell Tissue Res.* **292**, 503–512.

Fukuda M., Kanno E., Ogata Y., Saegusa C., Kim T., Loh Y. P. and Yamamoto A. (2003) Nerve growth factor-dependent sorting of synaptotagmin IV protein to mature dense-core vesicles that undergo calcium-dependent exocytosis in PC12 cells. *J. Biol. Chem.* **278**, 3220–3226.

Gil A., Viniegra S., Neco P. and Gutierrez L. M. (2001) Co-localization of vesicles and P/Q Ca^{2+}-channels explains the preferential distribution of exocytotic active zones in neuritis emitted by bovine chromaffin cells. *Eur. J. Cell. Biol.* **80**, 358–365.

Graham M. E., O'Callaghan D. W., McMahon H. T. and Burgoyne R. D. (2002) Dynamin-dependent and dynamin-independent processes contribute to the regulation of single vesicle release kinetics and quantal size. *Proc. Natl Acad. Sci. USA* **99**, 7124–7129.

Gutierrez L. M., Gil A. and Viniegra S. (1998) Preferential localization of exocytotic active zones in the terminals of neurite-emitting chromaffin cells. *Eur. J. Cell. Biol.* **76**, 274–278.

Haller M., Heinemann C., Chow R. H., Heidelberger R. and Neher E. (1998) Comparison of Secretory Responses as Measured by Membrane Capacitance and by Amperometry. *Biophys. J.* **74**, 2100–2113.

Han X., Wang C. T., Bai J., Chapman E. R. and Jackson M. B. (2004) Transmembrane segments of syntaxin line the fusion pore of Ca2+-triggered exocytosis. *Science* **304**, 289–292.

Hartmann J. and Lindau M. (1995) A novel Ca (2+)-dependent step in exocytosis subsequent to vesicle fusion. *FEBS Lett.* **363**, 217–220.

Islas-Suarez L., Gomez-Chavarin M., Drucker-Colin R. and Hernandez-Cruz A. (1994) Properties of the sodium current in rat chromaffin cells exposed to nerve growth factor in vitro. *J. Neurophysiol.* **72**, 1938–1948.

Jiménez N. and Hernández-Cruz A. (2001) Modifications of intracellular Ca^{2+} signaling during nerve growth factor-induced neuronal differentiation of rat adrenal chromaffin cells. *Eur. J. Neurosci.* **13**, 1487–1500.

Kawagoe K. T., Zimmerman J. B. and Wightman R. M., (1993) Principles of voltammetry and microelectrode surface states. *J. Neurosci. Meth.* **48**, 225–240.

Klingauf J. and Neher E. (1997) Modeling buffered Ca^{2+} diffusion near the membrane: implications for secretion in neuroendocrine cells. *Biophys. J.* **72**, 674–690.

Le R. and Esquenazi S. (2002) Astrocytes mediate cerebral cortical neuronal axon and dendrite growth, in part, by release of fibroblast growth factor. *Neurol. Res.* **24**, 81–92.

Livett B. G. (1984) Adrenal medullary chromaffin cells in vitro. *Physiol. Rev.* **64**, 1103–1161.

Llinas R. R., Sugimori M. and Silver R. B. (1995) The concept of calcium concentration microdomains in synaptic transmission. *Neuropharm.* **34**, 1443–1451.

Machado J. D., Segura F., Brioso M. A. and Borges R. (2000) Nitric oxide modulates a late step of exocytosis. *J. Biol. Chem.* **275**, 20 274–20 279.

Martin T. F. (2003) Tuning exocytosis for speed: fast and slow modes. *Biochim. Biophys. Acta* **1641**, 157–165.

McCarthy K. D. and De Vellis J. (1980) Preparation of separate astroglial and oligodendroglial cell cultures from rat cerebral tissue. *J. Cell Biol.* **85**, 890–902.

Meisinger C., Hertenstein A. and Grothe C. (1996) Fibroblast growth factor receptor 1 in the adrenal gland and PC12 cells: developmental expression and regulation by extrinsic molecules. *Brain. Res. Mol. Brain. Res.* **36**, 70–78.

Mendoza I. E., Schmachtenberg O., Tonk E., Fuentealba J., Díaz-Raya P., Lagos V. L., García A. G. and Cárdenas A. M. (2003) Depolarization-induced ERK phosphorylation depends on the cytosolic Ca^{2+} level rather than on the Ca^{2+} channel subtype of chromaffin cells. *J. Neurochem.* **86**, 1477–1486.

Mosharov E. V. and Sulzer D. (2005) Analysis of exocytotic events recorded by amperometry. *Nat. Meth* **2**, 651–658.

Neher E. (1998) Vesicle pools and Ca2+ microdomains: new tools for understanding their roles in neurotransmitter release. *Neuron* **20**, 389–399.

Parsons T. D., Coorssen J. R., Horstmann H. and Almers W. (1995) Docked granules, the exocytic burst, and the need for ATP hydrolysis in endocrine cells. *Neuron* **15**, 1085–1096.

Patterson P. H. (1990) Control of cell fate in a vertebrate neurogenic lineage. *Cell* **62**, 1035–1038.

Rudge J. S., Alderson R. F., Pasnikowski E., McClain J., Ip N. Y. and Lindsay R. M. (1992) Expression of Ciliary Neurotrophic Factor and the Neurotrophins-Nerve Growth Factor, Brain-Derived Neurotrophic Factor and Neurotrophin 3-in Cultured Rat Hippocampal Astrocytes. *Eur. J. Neurosci.* **4**, 459–471.

Sakai T. (1980) Relation between thickness and interference colors of biological ultrathin section. *J. Electron. Microsc. (Tokyo)* **29**, 369–375.

Scepek S., Coorssen J. R. and Lindau M. (1998) Fusion pore expansion in horse eosinophils is modulated by Ca^{2+} and protein kinase C via distinct mechanisms. *EMBO J.* **17**, 4340–4345.

Schober A., Arumae U., Saarma M. and Unsicker K. (2000) Expression of GFR alpha-1, GFR alpha-2, and c-Ret mRNAs in rat adrenal gland. *J. Neurocytol.* **29**, 209–213.

Schroeder T. J., Borges R., Finnegan J. M., Pihel K., Amatore C. and Wightman R. M. (1996) Temporally resolved, independent stages of individual exocytotic secretion events. *Biophys. J.* **70**, 1061–1068.

Segura F., Brioso M. A., Gómez J. F., Machado J. D. and Borges R. (2000) Automatic analysis for amperometrical recordings of exocytosis. *J. Neurosci. Meth.* **103**, 151–156.

Suter-Crazzolara C., Lachmund A., Arab S. F. and Unsicker K. (1996) Expression of neurotrophins and their receptors in the developing and adult rat adrenal gland. *Brain Res. Mol. Brain Res.* **43**, 351–355.

Tischler A. S., Riseberg J. C., Hardenbrook M. A. and Cherington V. (1993) Nerve growth factor is a potent inducer of proliferation and neuronal differentiation for adult rat chromaffin cells in vitro. *J. Neurosci.* **13**, 1533–1542.

Unsicker K., Skaper S. D. and Varon S. (1985) Developmental changes in the responses of rat chromaffin cells to neuronotrophic and neurite-promoting factors. *Dev. Biol.* **111**, 425–433.

Wang C. T., Grishanin R., Earles C. A., Chang P. Y., Martin T. F., Chapman E. R. and Jackson M. B. (2001) Synaptotagmin modulation of fusion pore kinetics in regulated exocytosis of dense-core vesicles. *Science* **294**, 1111–1115.

Wightman R. M., Jankowski J. A., Kennedy R. T., Kawagoe K. T., Schroeder T. J., Leszczyszyn D. J., Near J. A., Diliberto E. J. Jr. and Viveros O. H. (1991) Temporally resolved catecholamine spikes correspond to single vesicle release from individual chromaffin cells. *Proc. Natl. Acad. Sci. USA* **88**, 10 754–10 758.

Xin Q. and Wightman R. M. (1997) Enzyme modified amperometric sensors for choline and acetylcholine with tetrathiafulvalene tetracyanoquinodimethane as the electron-transfer mediator. *Anal. Chim. Acta* **341**, 43–51.

Yoo S. H., You S. H. and Huh Y. H. (2005) Presence of syntaxin 1A in secretory granules of chromaffin cells and interaction with chromogranins A and B. *FEBS Lett.* **579**, 222–228.

